IOPscience iopscience.iop.org

Home Search Collections Journals About Contact us My IOPscience

Numerical simulations of the four-dimensional Edwards-Anderson spin glass with binary couplings

This article has been downloaded from IOPscience. Please scroll down to see the full text article.

1999 J. Phys. A: Math. Gen. 32 7447

(http://iopscience.iop.org/0305-4470/32/43/301)

View the table of contents for this issue, or go to the journal homepage for more

Download details:
IP Address: 171.66.16.111
The article was downloaded on 02/06/2010 at 07:48

Please note that terms and conditions apply.

J. Phys. A: Math. Gen. **32** (1999) 7447–7461. Printed in the UK PII: S0305-4470(99)03878-0

Numerical simulations of the four-dimensional Edwards–Anderson spin glass with binary couplings

Enzo Marinari and Francesco Zuliani

Dipartimento di Fisica and INFN, Università di Cagliari, Cittadella Universitaria, SP Monserrato-Sestu Km 0.7, 09042 Monserrato (CA), Italy

E-mail: Enzo.Marinari@ca.infn.it and Francesco.Zuliani@ca.infn.it

Received 30 April 1999

Abstract. We present numerical results that allow a precise determination of the transition point and of the critical exponents of the four-dimensional Edwards–Anderson spin glass with binary quenched random couplings. We show that the low-temperature phase undergoes replica symmetry breaking. We obtain results on large lattices, up to a volume $V = 10^4$: we use finite-size scaling to show the relevance of our results in the infinite volume limit.

1. Introduction

The question of whether short-range Edwards–Anderson (EA) spin glasses share the remarkable features of the infinite-range Sherrington–Kirkpatrick (SK) model [1] is still an open one. In this work we present Monte Carlo (MC) simulations of the four-dimensional (4D) EA ising spin Glass [2–8] with a bimodal distribution of the quenched couplings, performed on large lattice volumes (thanks to the tempering and parallel tempering simulation technique [9, 10]), with a large number of samples, and down to low values of the temperature T. In this way we are able to obtain detailed information about the nature of the transition, to determine with good precision critical temperature and exponents, and to give strong evidence supporting the fact that the low-T phase is mean-field-like. A great deal of effort has gone into ensuring the reliability of the data on delicate issues such as thermalization checks and consistency of data analysis.

The paper is organized as follows: first, we describe the model and the parameters of our MC simulation. We then present data related to the Binder cumulant and to the determination of T_c and ν. By analysing the overlap susceptibility we determine the value of η. Finally, we discuss in detail the probability distribution of the overlap $P(q)$. We present, among other things, evidence for the non-triviality of a single sample $P_J(q)$ and for a non-zero value of the position of the maximum of $P(q)$, q_{max}, in the thermodynamic limit.

2. The numerical simulation

It is very difficult to run a reliable numerical simulation of finite-dimensional spin glasses. The main reason for such difficulties is the presence of many meta-stable states (responsible for aging effects as well as for many other peculiarities of spin glasses [1]). The MC dynamics gets easily trapped, and the system only probes a restricted part of phase space.

0305-4470/99/437447+15$30.00 © 1999 IOP Publishing Ltd

Table 1. Parameters of the tempered MC runs.

L	Thermalization	Equilibrium	Samples	N_β	δT	T_{min}	T_{max}
3	100 000	100 000	3200	17	0.1	1.2	2.8
4	100 000	100 000	2944	17	0.1	1.2	2.8
5	100 000	100 000	1920	17	0.1	1.2	2.8
6	100 000	100 000	1120	33	0.05	1.2	2.8
8	100 000	100 000	1376	33	0.05	1.2	2.8
10	150 000	150 000	512	56	0.04	1.2	3.4

Many algorithmic solutions have been proposed to improve the speed of thermalization of these systems. All these techniques are related to density scaling methods (see [10] for a review and references): we use here the maybe simplest implementation of these ideas, parallel tempering [9], where a number of configurations of the system are allowed to exchange their temperature (for multi-canonical methods, that are strongly related and have in principle an even wider range of applicability, see, for example, [11]). Thanks to parallel tempering we have been able to thermalize systems of volume $V = 10^4$ down to $T \simeq 1.2(0.6T_c)$.

We study the 4D EA Ising spin glass with binary couplings, with Hamiltonian

$$H \equiv -\sum_{\langle i,j\rangle} J_{ij}\sigma_i\sigma_j \tag{1}$$

where the sum runs over nearest neighbouring sites, the σ_i are ± 1 Ising spins, and the couplings are quenched variables drawn with probability $\frac{1}{2}$ among the two values $\{-1, +1\}$. The *overlap* among two different systems is defined as

$$q^{\alpha,\beta} \equiv \frac{1}{V}\sum_i \sigma_i^\alpha \sigma_i^\beta \tag{2}$$

where α and β denote two configurations of the system in the same realization of the quenched disorder. The overlap probability distribution for a given sample is

$$P_J(q) \equiv \langle \delta(q - q^{\alpha,\beta})\rangle \tag{3}$$

where $\langle \ldots \rangle$ denotes the usual Gibbs average. Its average over samples is

$$P(q) \equiv \overline{P_J(q)} \tag{4}$$

and its moments are defined as

$$q^{(n)} = \overline{\langle q^n\rangle} = \int \mathrm{d}q\, q^n P(q). \tag{5}$$

We always denote by $\langle \ldots \rangle$ the thermal averages and by $\overline{\ldots}$ the disorder averages.

Our simulations have been performed on a set of workstations, using a multi-spin-coding program that was inspired by the work of [12]. We have selected the parameters of our MC and parallel tempering runs such to guarantee a complete thermalization of the measured observables. We will discuss this issue in some detail.

Table 1 summarizes the relevant parameters used in the simulation: we give among others the number of thermalization steps, of measurements steps, the number of different disorder realizations and the temperature ranges investigated by tempering. Temperature values have been chosen to be uniformly spaced in the interval between T_{min} and T_{max}.

We have used different methods to verify that we have correctly thermalized the systems. Using 'parallel tempering', one is actually performing a generalized Markov chain where systems at different temperatures are allowed to 'move' in temperature–space too. A necessary condition for the Markov chain to be effective in de-correlating different measurements is the

fact that each system spans at least a few times all the allowed temperature range during the simulation. In this respect we check *a posteriori* that the probability of swapping temperature has been of the order of 0.5 (ensuring in this way that a single system did not get stuck at a specific value of T) and that the histogram counting the time that each system has spent at each temperature is fairly flat. This requirement is fulfilled in all our simulations, for all T and L values.

Another very strong check of thermalization is the fact that the single sample $P_J(q)$ is symmetric in the limits of the statistical significance of the histogram. This is very well verified as can be seen, for example, in figure 12 where we plot $P_J(q)$ for selected samples.

3. The Binder parameter, T_c and ν

We start by discussing the overlap Binder parameter. We will use it to qualify the phase transition, and to determine the critical temperature and the first of the critical exponents, ν. We will use and describe different methods to compute the quantities we are interested in. Our statistical sample of configurations is a large sample, and our set of data precise (even as far as the dependence over the lattice volume V is concerned): we will show that different analysis styles give compatible (precise) results.

We define the usual overlap Binder parameter as

$$g = \frac{1}{2}\left(3 - \frac{\overline{\langle q^4\rangle}}{\overline{\langle q^2\rangle}^2}\right). \tag{6}$$

The Binder parameter is an adimensional quantity, and its value at the critical point is universal. Close to T_c its leading behaviour is

$$g(L, T) \simeq \bar{g}(L^{\frac{1}{\nu}}(T - T_c)). \tag{7}$$

In usual ferromagnetic systems the infinite volume limit of the magnetization Binder cumulant is zero in the warm phase (where the distribution of the order parameter is Gaussian) and one in the broken phase: for a spin glass with replica symmetry breaking (RSB) and hence a non-trivial distribution of the overlap order parameter, the transition is signalled by a non-trivial value of g in the broken phase (in the warm phase one expects an infinite volume limit of zero). In both cases the location of T_c is signalled by the crossing of the curves of g versus T for different values of the lattice size L (asymptotically for large L): large L curves are lower for $T > T_c$ and higher for $T < T_c$. We show in figure 1 g versus T for different L values. The crossing point is close to $T \simeq 2$ for all lattice values, and the value of the Binder cumulant at criticality, g_c, is close to 0.45. Also, error analysis has been a sensitive issue. We have always used a jack-knife or a bootstrap error analysis [13] *directly* on the fitted parameters to determine errors. Still, one has to keep in mind that statistical errors come together with systematic errors, due to the functional form one decides to try to fit (typically the asymptotic scaling form, that on finite-size lattices is affected by power corrections). The two types of errors have to be kept under control separately.

In figure 1 the crossing of the different g_L curves is very clear. It is interesting to stress the difference with the 3D case [14], where the crossing at T_c looks more like a merging of the different curves. The 3D case is (very) close to the lower critical dimension, while in four dimensions we are in a safe region: potentially this is important to make the physical picture easier to understand.

Let us discuss a first naive approach to the data. By looking at the crossing of the curves $g_L(T)$ versus T for different $(L, L + 1)$ values one sees that one cannot extract a systematic dependence of the crossing point (and hence of the estimate of the effective critical temperature

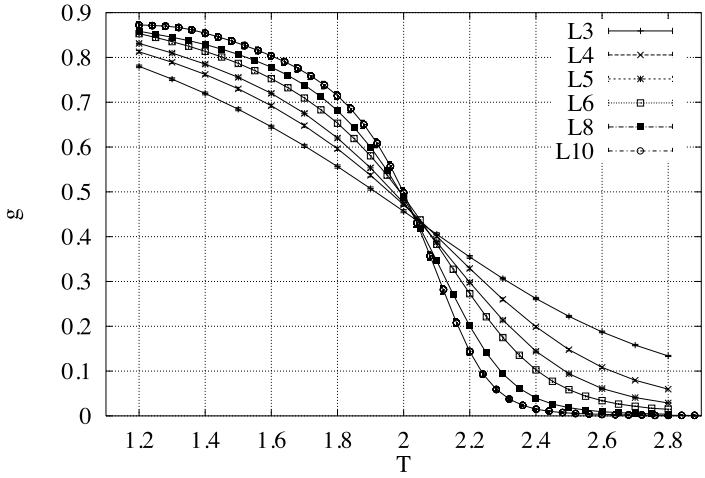

Figure 1. Binder parameter g versus T, for different values of the linear lattice size L (see the caption in the plot).

$T_c(L, L+1)$) over L. Any systematic trend is smaller than the statistical error (maybe just showing a systematic average decrease of the estimate $T_c(L, L+1)$ when going from smaller to larger L values). The preferred value of T_c is slightly larger than 2.00. A first naive estimate of ν can be done by linearizing $g_L(T)$ around the estimate we have given for T_c, and by evaluating the logarithm of the slope ratio (divided by the logarithm of the two lattice sizes ratio, $\log(\frac{L}{L+1})$). With this method, one gets a first estimate for a set of effective exponents $\nu(L, L+1)$. Here too, one cannot distinguish any clear strong dependence over the lattice size: the error one gets on ν is completely correlated to the variation of the estimate of T_c. For larger T_c one estimates a lower value of ν, while for lower estimates of T_c one gets larger estimates for ν. The error is dominated by this effect. The estimate for ν is close to one.

To get a reliable estimate of T_c and of ν we have used two methods of analysis of g (see, for example, the discussion of the analysis of [14, 15]). In the first approach we linearize the data close to T_c (for all L values) and we run a global fit to all data: we fit T_c and ν for the two-variable function $g_L(T)$ (as we said, linearized close to T_c). We use data in a T range around the interval 1.9–2.1. We estimate the errors over the fit parameters (T_c and ν) by a jack-knife approach [13]: we repeat the fit approximately K times over a subsample of the data containing all of our statistical sample but a fraction $\frac{1}{K}$. The error is estimated by looking at fluctuations of the results of the K fits, and by accounting for the fact they are correlated [13]. We also repeat the fits by discarding the smaller L values, to check if we can observe any systematic drift (again with good accuracy the average value of the result does not seem to depend systematically over the L range selected). Results are very stable, and the value we estimate for ν systematically comes out to be close to 1.10.

In the second approach, that can have different variations, one only uses data in the warm phase. This method leads to a smaller statistical error, that is balanced from a larger systematic incertitude (since we only select data at a given distance from T_c, and approaching T_c leads to a systematic drift of the estimate). In this case we start by selecting a threshold value for g, $g^* \leqslant g_c$. We start with low values of g^*, and we approach g_c from below: we cannot get too close to g_c or the merging of the curves for different sizes makes the error over the measurement too large (we use values of g^* from 0.2 to 0.4). We use a polynomial fit to interpolate the data for $g(T)$, at different L values. We have decided to use a polynomial of degree four (we

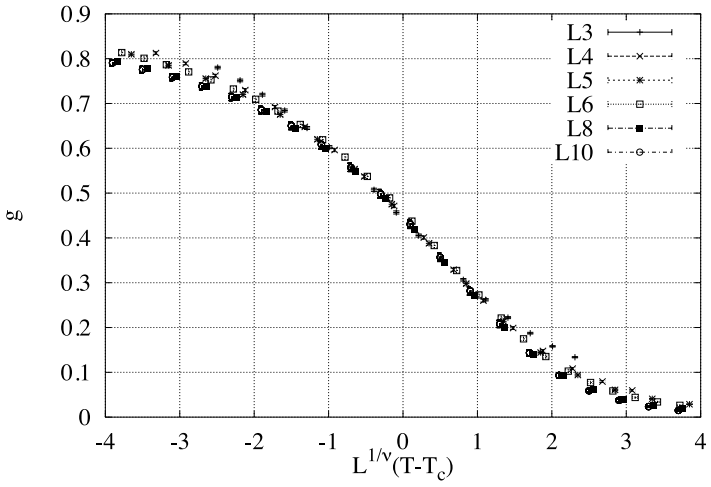

Figure 2. g versus $L^{\frac{1}{\nu}}(T - T_c)$, with $\nu = 1.0$ and $T_c = 2.03$.

have checked that it guarantees stable fits and consistent results), and we fit a T range in the critical region (for $L = 3$ we use the data in the T range 1.5–2.8, for $L = 10$ we use the range 1.88–2.16). We now define $T_c(L, g^*)$ as the crossing point of the fitted polynomial with the horizontal line at g^*, and ν^* as

$$\lim_{L\to\infty} T_c(L, g^*) = T_c(g^*) + \frac{A}{L^{\frac{1}{\nu^*}}} \tag{8}$$

when $g^* \to g_c$ $\nu^* \to \nu$. If g^* is too small violations of scaling are dominant, while if one approaches too much g_c the merging of the g curves makes the error over the determination of ν^* overwhelming. The errors have been estimated by using a *bootstrap* approach (very similar in spirit to the jack-knife technique, see [13]): one emulates fake sets of data with a Gaussian distribution around the real measurements, fits these multiple sets of fake data and compute the errors over the fit parameter.

We note finally that we have also used a variation of this second method, described in [14], based on the direct analysis of the derivative of g with respect to T. This method also gives results that are compatible with others.

Our final estimates, averaged over the results obtained using these different approaches, are

$$T_c = 2.03 \pm 0.03 \tag{9}$$

and

$$\nu = 1.00 \pm 0.10. \tag{10}$$

In the rest of this paper we will use these two values as our best estimates of T_c and ν. We show in figure 2 the data for $g_L(T)$ rescaled by using these two values: the scaling turns out to be very satisfactory.

4. The Overlap Susceptibility and η

The determination of the overlap susceptibility, χ_q, provides various possible ways to determine the exponent η (and hence of the exponent γ). In a spin glass in the RSB phase the overlap

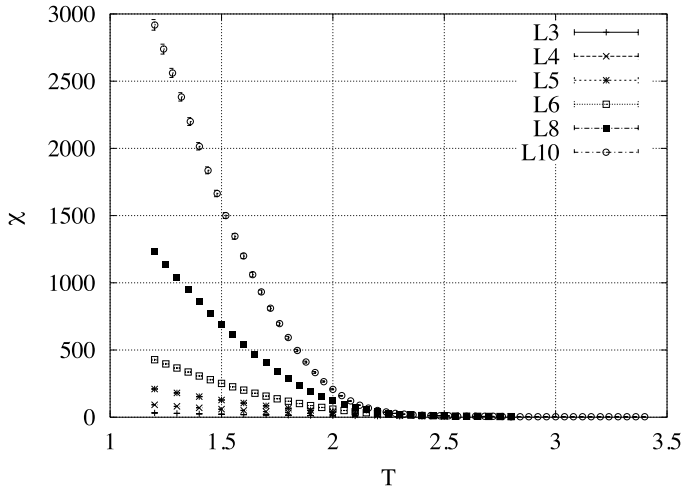

Figure 3. Overlap susceptibility χ_q versus T, for different L values.

susceptibility

$$\chi_q \equiv V\langle q^2\rangle \tag{11}$$

is expected to diverge for all values of $T \leqslant T_c$. We show χ_q versus T in figure 3.

The first method is based on the fact that we expect that at $T = T_c$

$$\chi_q(L, T = T_c) \simeq L^{2-\eta}. \tag{12}$$

We use a linear interpolation of the data in the region close to T_c. As in the case of g, the error in the estimate is mainly related to the choice of T_c. The fit at $T = 2.03$ by using $L > 3$ gives an estimate of 0.28.

In the second method we use data where $L \gg \xi$. We go as close to T_c as possible, under the condition that data on our larger lattice ($L = 10$) coincide, in our statistical accuracy, with the ones at $L = 8$. Here we expect that

$$\chi_q(T) \simeq (T - T_c)^{-(2-\eta)\nu}. \tag{13}$$

We can use data down to $T = 2.5$ (i.e. at a $\Delta T \simeq 0.5$ from T_c), where finite-size effects start to be sizable even at $L = 10$. We show our best fit (in a T interval of $= 0.2$) in figure 4. In this region we have a stable fit, with η close to -0.4. Even if this second measurement is not very precise (we have to stay quite far from the critical region) it is interesting that we get a coherent determination of η, by using a completely different scaling region than in the former analysis (the new analysis also depends on the value of ν we have determined by using g).

The last approach we use for determining η is based on the analysis of the scaling properties of the distribution probability $P(q)$ of the overlap order parameter q in the region $q \simeq 0$ at $T = T_c$. We analyse the behaviour of $P(q)$ in the next section, but for now we discuss the scaling of $P(0)$ of T_c in order to define our determination of η. At $T = T_c$ we expect

$$P(q \simeq 0) \simeq L^{\frac{d-2+\eta}{2}} \tag{14}$$

i.e. in $d = 4$ a scaling with $L^{\frac{2+\eta}{2}}$. We find a very good best fit (we do not include the $L = 3$ data), with an η value close to -0.3.

By considering all the methods we have discussed in this section we give our final estimate

$$\eta = -0.30 \pm 0.05 \tag{15}$$

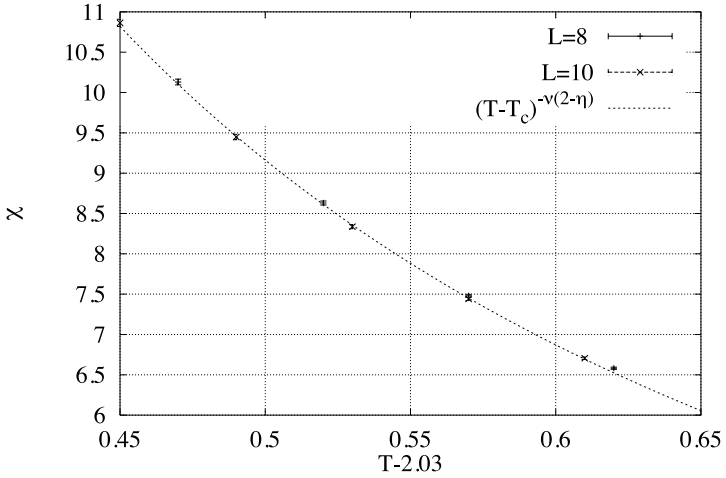

Figure 4. Best fit to the overlap susceptibility χ_q versus $T - T_c$, at $T > T_c$.

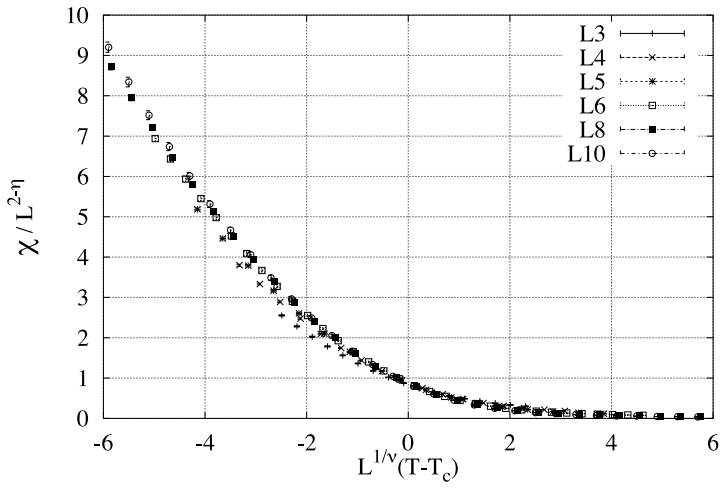

Figure 5. Rescaled overlap susceptibility $\frac{\chi_{SG}}{L^{2-\eta}}$ versus $L^{\frac{1}{\nu}}(T - T_c)$, with $T_c = 2.03$, $\nu = 1.0$ and $\eta = -0.30$.

that we will use in the rest of our analysis. In figure 5 we plot χ_q rescaled by using our best fits. The rescaling works fine.

Let us also notice that we have a good agreement with the results reported in [7] for the 4D EA model with Gaussian couplings. There the authors find $\nu \simeq 1.06$ and $\eta \simeq -0.35$. Universality seems to work.

5. $P(q)$

In sections 3 and 4 we have shown that the 4D EA model undergoes a phase transition, and we have determined its location and the critical exponents. Now we will try to qualify it in better detail, by determining and analysing the probability distribution of the order parameter, $P(q)$.

In figure 6 we show our average $P(q)$ (averaged over the different disorder realizations)

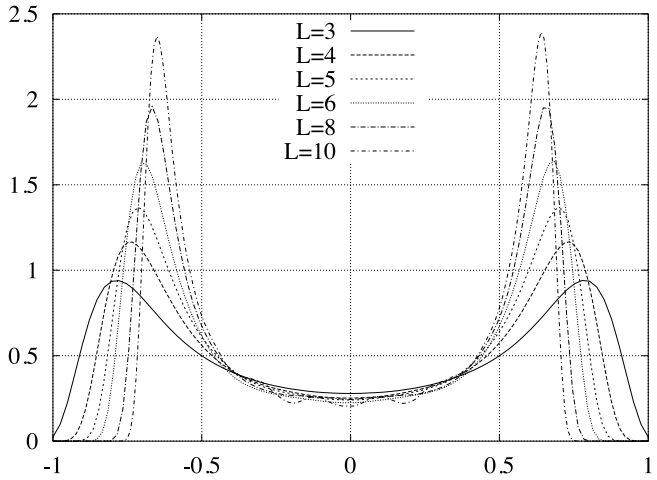

Figure 6. $P(q)$ at $T = 1.2$ (broken phase), for different lattice sizes.

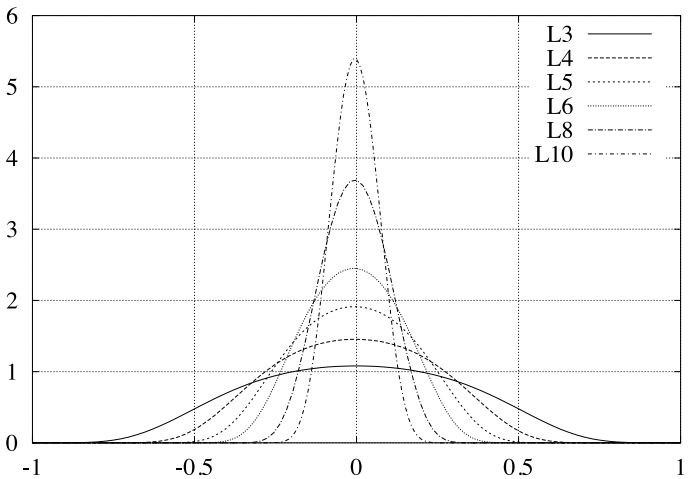

Figure 7. $P(q)$ at $T = 2.2$ (warm phase), for different lattice sizes.

at $T = 1.2 < T_c$. When increasing the lattice size the peak where $P(q)$ is maximum shifts to lower q values: to show that there is a phase transition to a phase with a non-zero expectation value of q we have to show that the peak does not go to $q = 0$ when $L \to \infty$. The *plateau* of $P(q)$ for $q \simeq 0$ does not lower when increasing L, as we will discuss in more detail in the following. We remind the reader that in the RSB Parisi mean field scenario the $P(q)$ is (in zero magnetic field) a non-trivial function, that in the infinite volume limit is formed by a δ function at $q = q_{EA}$ and by a regular part that extends down to $q = 0$. In contrast, if the broken phase has the same structure of the one of an ordered ferromagnet $P(q)$ has to become asymptotically the sum of two δ functions at $\pm q_{EA}$.

For the sake of comparison we show in figure 7 what happens in the warm phase, where the average $P(q)$ shrinks to a Gaussian distribution around $q = 0$, when $L \to \infty$.

In figure 8 we compare $P(q)$ at different values of T on the same lattice size. From the single-peaked shape at high T one gets a clear double-peaked structure, with a clear *plateau*

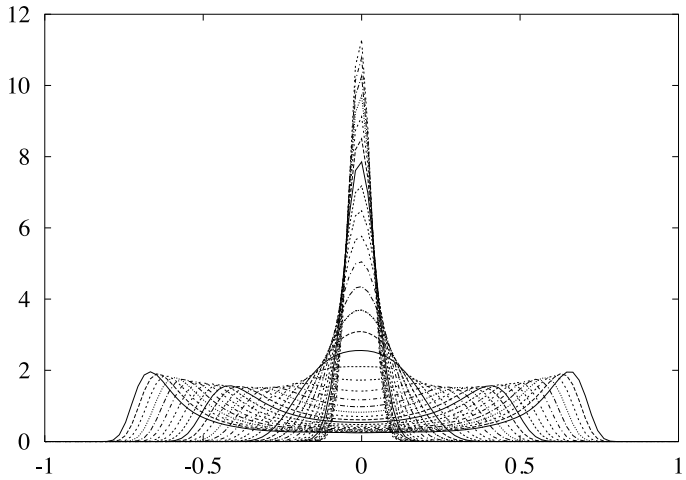

Figure 8. $P(q)$ at $L = 8$, for all values of T. From a single peak in $q = 0$ to a continuous part and double peak at large q for increasing T.

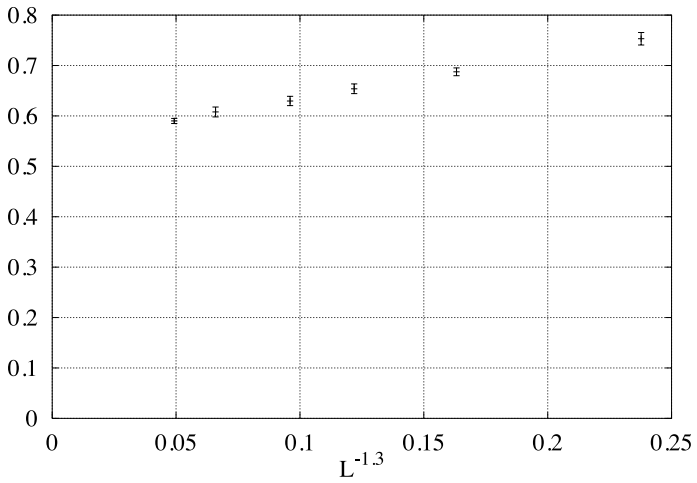

Figure 9. q_{max} versus $L^{-1.3}$.

at low q, in the low-T region.

As we have said, in order to establish that we have a real phase transition in the infinite volume limit we have to show that the value of $q = q_{max}$ where $P(q)$ is maximum does not go to zero. We start by plotting in figure 9 q_{max} versus $L^{-1.3}$ (the exponent 1.3 comes from our best fit, see later). It is easy to see that an asymptotic value $q_{max} = 0$ seems implausible.

Making this last statement more quantitative needs a more careful analysis. In order to do that we fit

$$q_{max}(L) = q_{max}(\infty) + \frac{A}{L^{\alpha}} \tag{16}$$

both with $q_{max}(\infty) = 0$ and by allowing it a non-zero value. In figure 10 we plot the values of q_{max} versus L and the results of the two best fits, one with a fitted value of $q_{max}(\infty)$ and the second with fixed $q_{max}(\infty) = 0$. This second fit is clearly unsuitable, and it has a very high

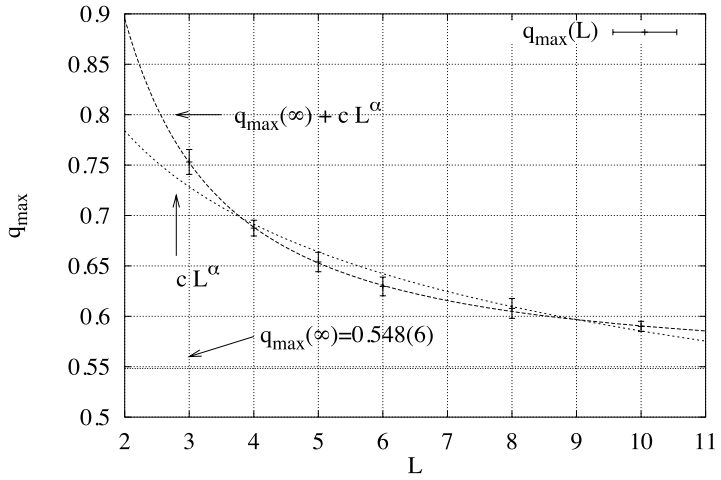

Figure 10. q_{max} versus L and our two best fits.

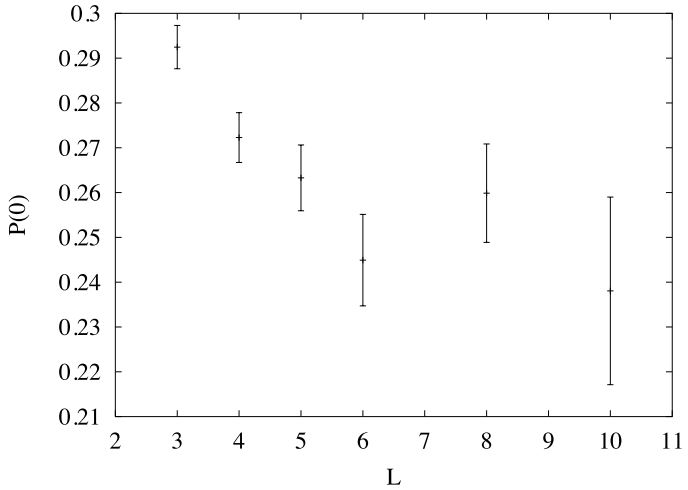

Figure 11. $P(q \simeq 0)$ versus L. $T = 1.2$.

value of χ^2. In the first fit we get

$$q_{max}(\infty) = 0.548 \pm 0.006 \tag{17}$$

which is our best estimate for the position of the δ function at q_{EA} in the infinite volume limit. We estimate $\alpha = 1.3 \pm 0.1$ (in the fit with a zero asymptotic value one finds the very small value $\alpha \simeq 0.2$).

In figure 11 we show the value of $P(q)$ close to $q = 0$ (averaged over a small q range, where $P(q)$ is remarkably constant, in order to diminish statistical fluctuations) as a function of L. One cannot observe any statistically significant decrease of this value for increasingly large lattice volume (there is a small decrease only for small volumes). The most plausible implication of this evidence is that the system has many stable states, and that the cold T phase is characterized by RSB (even if it has to be stressed that this evidence is not as strong as that implied by figure 10).

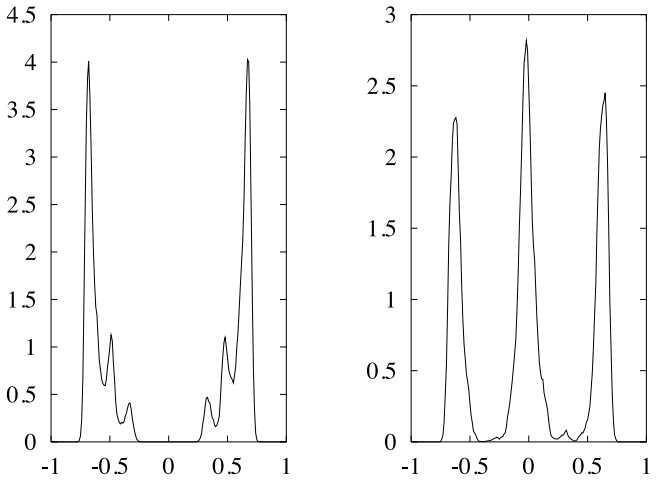

Figure 12. $P_J(q)$ for selected samples. $T = 1.2$, $L = 10$.

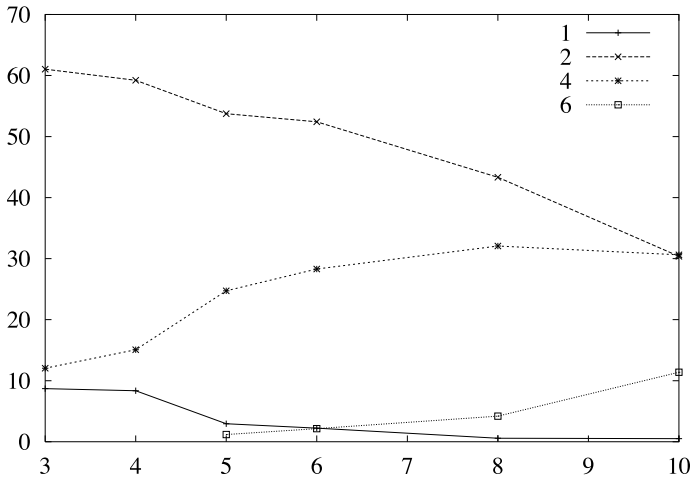

Figure 13. Percentage of disorder configurations such that $P_J(q)$ has 1, 2, 4 and 6 peaks versus L. The number of configurations with a complex phase space ($P_J(q)$ with many peaks) increases strongly with L.

In figure 12 we plot $P_J(q)$ for selected samples, at $T = 1.2$, $L = 10$. One can see that they are very complex distributions: such a pattern is typically related to the presence of many states (it should be noticed, however, that the small side peaks are not always there because of the presence of a real state).

To be more quantitative we have measured the percentage of disorder configurations such that $P_J(q)$ has 1, 2, 4 and 6 peaks versus L, and we plot it in figure 13. The number of configurations with a complex phase space ($P_J(q)$ with many peaks) increases strongly with L. We use this evidence to rule out the picture of a *modified droplet model*, that has been discussed, among others, in [16] and in references therein. The picture of the modified droplet models implies that for each realization of the quenched disorder there are (in the cold phase) only two ground states, but that the value of q_{EA} (i.e. the support of the δ function that constitutes

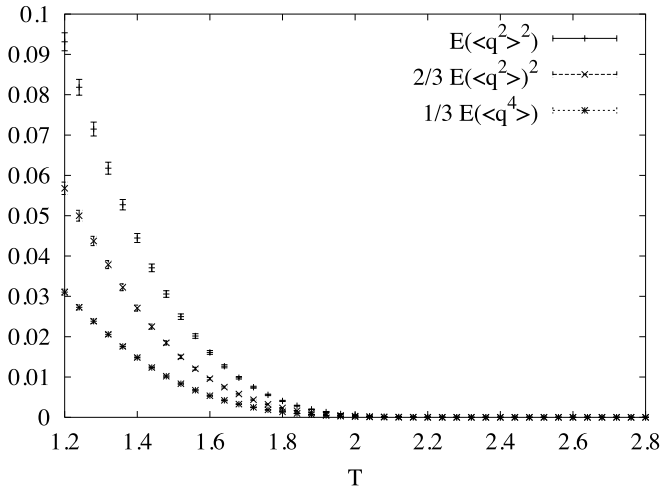

Figure 14. $\overline{\langle q^2\rangle^2}$, $\overline{\langle q^2\rangle}^2$ and $\overline{\langle q^4\rangle}$ versus T.

the $P_J(q)$) depends on the sample. Here, in contrast, the number of states for a given sample is strongly increasing with L (and with decreasing T).

6. Sum rules

In this section we discuss another important feature of the broken phase of the 4D EA model. The starting point for this analysis can be, for example, the relation

$$\overline{\langle q^2\rangle^2} = \tfrac{2}{3}\overline{\langle q^2\rangle}^2 + \tfrac{1}{3}\overline{\langle q^4\rangle}. \tag{18}$$

This is one of a set of relations that are valid in the mean field theory of spin glasses [17]. The work contained in [18] has established numerically that these relations are also satisfied with good accuracy in finite-dimensional spin glasses. Following these findings a rigorous and theoretical analysis has improved our understanding of such a set of sum rules [19–22]: they are strongly related to the ultrametric properties of the phase space.

First of all we show evidence that the relation (18) has a non-trivial content in the low-T phase (in the high-T phase it is satisfied in the form $0 = 0$). Figure 14 shows that the values of the three quantities involved in (18) are significantly different from zero below T_c (we have already shown in better detail that the infinite volume of such quantities is non-zero).

In figure 15 we show the difference between the left- and the right-hand side of (18). The two contributions cancel out with good accuracy (to three significant figures), and asymptotically for large lattice size the difference extrapolates to zero.

Another possible way to visualize the result is to plot the ratio of the left- and the right-hand side. As figure 16 shows, for T below T_c we get identically one, while for $T \to \infty$ we get the value $\frac{3}{5}$, expected for a Gaussian $P(q)$.

We have also fitted the difference plotted in figure 15, for various values of temperatures $T < T_c$: in all cases a fit to an asymptotic zero value with power corrections works very well, and the exponent of the corrections is close to 3 for all T values. As an example we plot the data together with the best fit for $T = 1.4$ in figure 17.

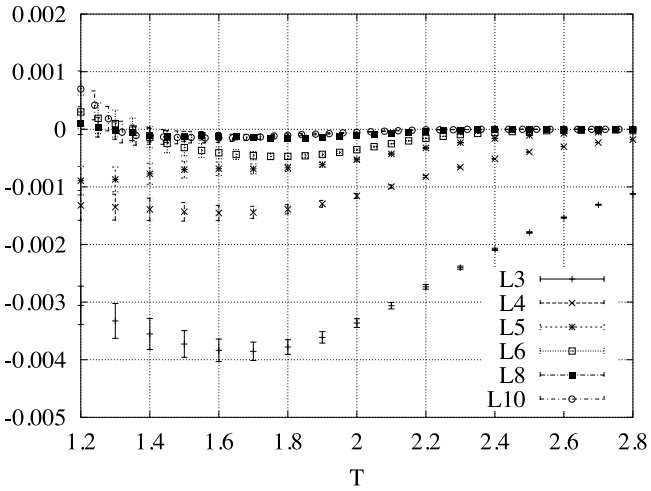

Figure 15. The left- minus the right-hand side of equation (18) versus T.

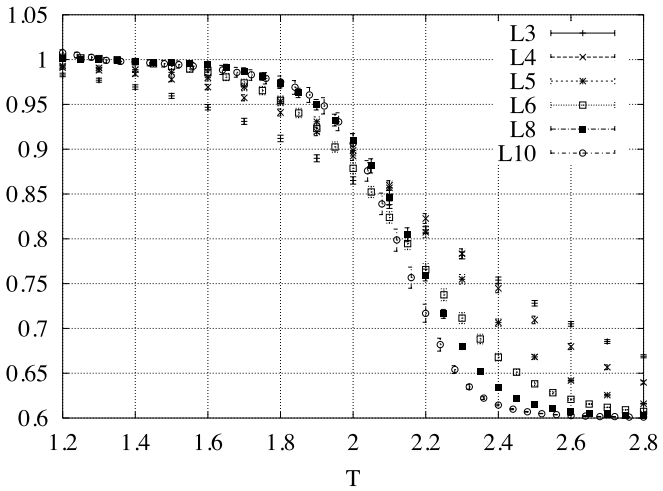

Figure 16. Ratio of the left- and right-hand side of equation (18) versus T.

7. Conclusions

In this paper we have been able to give strong evidence for mean field behaviour of the 4D Ising spin glass with binary couplings. Life in the 4D model is easier than in three dimensions, where even after a large number of intense numerical simulations the evidence for a phase transition is still slightly marginal (even if, at this point, it appears convincing enough). In our case already the crossing of the Binder cumulants is the very clear signature of a typical phase transition (as opposed to the quasi-merging, quasi-Kosterlitz–Thouless behaviour of the 3D case). It is clear that the 3D case is very close to the lower critical dimension, and that observing the effects of the physical critical point there is dramatically difficult. Four dimensions are safer, and numerical simulations show that very clearly.

We have been able to determine critical exponents precisely, and to enter into the large

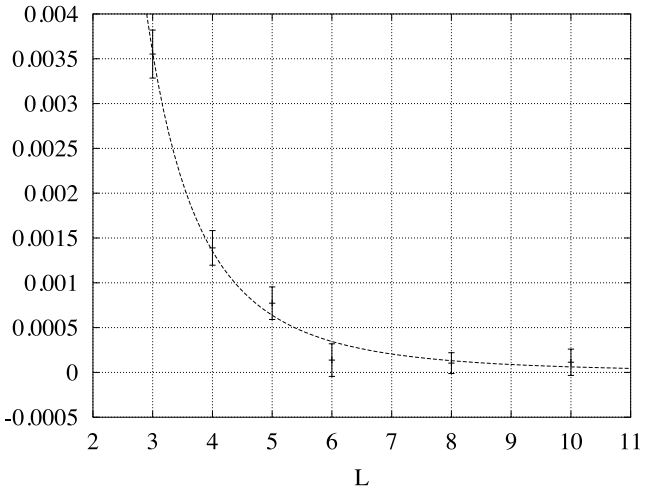

Figure 17. The left- minus the right-hand side of equation (18) versus L, at $T = 1.4$, and the best fit to a zero constant value with a simple power correction.

volume region with good accuracy. For example, we have been able to show that the peak of $P(q)$ does not go to $q = 0$ for increasing lattice size, and (with a slightly poorer accuracy and level of reliability) that the plateau at $q \simeq 0$ does not decrease with increasing lattice size. Also, we remind the reader that non-trivial sum rules are satisfied with very good accuracy. Therefore, things look quite clear in the 4D case.

Acknowledgments

We thank Giorgio Parisi, Federico Ricci-Tersenghi and Juan Ruiz-Lorenzo for a number of interesting discussions.

References

[1] Mezard M, Parisi G and Virasoro M A 1987 *Spin Glass Theory and Beyond* (Singapore: World Scientific)
[2] Bhatt R N and Young A P 1988 *Phys. Rev.* B **37** 5606
[3] Reger J D, Bhatt R N and Young A P 1990 *Phys. Rev. Lett.* **64** 1859
[4] Parisi G and Ritort F 1993 *J. Phys. A: Math. Gen.* **26** 6711
[5] Ciria J C, Parisi G and Ritort F 1993 *J. Phys. A: Math. Gen.* **26** 6731
[6] Badoni D, Ciria J C, Parisi G, Ritort F, Pech J and Ruiz-Lorenzo J J 1993 *Europhys. Lett.* **21** 495
[7] Parisi G, Ricci-Tersenghi F and Ruiz-Lorenzo J J 1996 *J. Phys. A: Math. Gen.* **29** 7943
(Parisi G, Ricci-Tersenghi F and Ruiz-Lorenzo J J 1996 *Preprint* cond-mat/9606051)
[8] Bernardi L W and Campbell I A 1997 *Phys. Rev.* B **56** 5271
(Bernardi L W and Campbell I A 1997 *Preprint* cond-mat/9704086)
[9] Marinari E and Parisi G 1992 *Europhys. Lett.* **19** 451
(Marinari E and Parisi G 1992 *Preprint* hep-lat/9205018)
Tesi M C, Janse van Rensburg E J, Orlandini E and Whillington S G 1996 *J. Stat. Phys.* **82** 155
Hukushima K and Nemoto K 1996 *J. Phys. Soc. Japan* **65** 1604
(Hukushima K and Nemoto K 1995 *Preprint* cond-mat/9512035)
[10] Marinari E 1998 Optimized MC methods *Advances in Computer Simulation* ed J Kertész and I Kondor (Berlin: Springer)
[11] Berg B A 1998 *Nucl. Phys. Proc. Suppl.* **63** 982 and references therein

[12] Rieger H 1992 Fast vectorized algorithm for the Monte Carlo simulation of the random field Ising model *Preprint* HLRZ 53/92, hep-lat/9208019
[13] Flyvbjerg H 1998 Error estimates on averages of correlated data in *Advances in Computer Simulation* ed J Kertész and I Kondor (Berlin: Springer)
[14] Marinari E, Parisi G and Ruiz-Lorenzo J J 1998 Phase structure of the three-dimensional Edwards–Anderson spin glass *Phys. Rev.* B **58** 14 852
(Marinari E, Parisi G and Ruiz-Lorenzo J J 1998 *Preprint* cond-mat/9802211)
[15] Iñiguez D, Parisi G and Ruiz Lorenzo J J 1996 *J. Phys. A: Math. Gen.* **29** 4337
(Iñiguez D, Parisi G and Ruiz Lorenzo J J 1996 *Preprint* cond-mat/9603083)
[16] Newman C M and Stein D L 1996 *Phys. Rev. Lett.* **76** 515 and references therein
[17] Mézard M, Parisi G, Sourlas N, Toulouse G and Virasoro M A 1984 *J. Physique* **45** 843
[18] Marinari E, Parisi G, Ritort F and Ruiz-Lorenzo J 1996 *Phys. Rev. Lett.* **76** 843
(Marinari E, Parisi G, Ritort F and Ruiz-Lorenzo J 1996 *Preprint* cond-mat/9508036)
[19] Guerra F 1996 *Int. J. Mod. Phys.* B **10** 1675
[20] Aizenman M and Contucci P 1998 *J. Stat. Phys.* **92** 765
(Aizenman M and Contucci P 1998 *Preprint* cond-mat/9712129)
[21] Parisi G 1998 On the probabilistic formulation of the replica approach to spin glasses *Preprint* cond-mat/9801081
[22] Marinari E, Parisi G, Ricci-Tersenghi F, Ruiz-Lorenzo J and Zuliani F 1999 Replica symmetry breaking in short range spin glasses: a review of the theoretical foundations and of the numerical evidence *Preprint* cond-mat/9906076 (submitted to *J. Stat. Phys.*)